

Mustafa Burak Yilmaz, Anja Klein, Lin Xiang, "Energy Minimization for UAV-Aided ISAC in a Cluttered Environment", in '*IEEE Global Communications Conference*', Cape Town, 2024.

©2024 IEEE. Personal use of this material is permitted. However, permission to reprint/republish this material for advertising or promotional purposes or for creating new collective works for resale or redistribution to servers or lists, or to reuse any copyrighted component of this works must be obtained from the IEEE.

Energy Minimization for UAV-Aided ISAC in a Cluttered Environment

Mustafa Burak Yilmaz, Anja Klein, and Lin Xiang

Communications Engineering Lab, Technical University of Darmstadt, Darmstadt, Germany

Email: {b.yilmaz, a.klein, l.xiang}@nt.tu-darmstadt.de

Abstract—This paper investigates integrated sensing and communication (ISAC) enabled by a multi-antenna unmanned aerial vehicle (UAV) for simultaneously serving multiple downlink communication users and sensing multiple targets during flight. Unlike previous studies, we consider target sensing in a cluttered environment where echoes backscattered by the clutter can interfere and significantly degrade the ISAC performance. To mitigate the impact of the clutter, we jointly optimize the UAV’s transmit beamforming, sensing scheduling and trajectory design for minimizing its total energy consumption while meeting required data rates for communication and signal-to-clutter-plus-noise ratio (SCNR) in sensing. The formulated problem is a nonconvex mixed-integer nonlinear program (MINLP). We uncover a hidden convexity in the optimization of the continuous variables with discrete variables fixed. This enables us to propose a novel low-complexity and high-quality solution by reformulating the original problem as a multi-stage dynamic programming (DP) and solving the discrete and continuous variables using the one-step lookahead rollout (OSLR) algorithm from approximate DP and the semidefinite programming from convex optimization, respectively. Simulation results show that clutter interference has a non-negligible impact on ISAC and should be judiciously mitigated. Meanwhile, our proposed optimization algorithm achieves significant energy savings for UAV-aided ISAC in cluttered environments, compared with a clutter-aware non-OSLR-based baseline scheme.

I. INTRODUCTION

Integrated sensing and communication (ISAC) is an advanced physical layer technology that enables simultaneous sensing and communication using the same spectrum and transmitter hardware [1]. Recently, there has been growing interest in utilizing unmanned aerial vehicles (UAVs) to deploy on-demand three-dimensional (3D) ISAC functionality within sixth-generation (6G) wireless networks [2], [3]. UAV-enabled ISAC is expected to provide reliable communication and sensing capabilities, even in environments with disrupted or limited network infrastructure, making it pivotal for both routine operations and emergency scenarios [4].

However, successfully deploying UAVs as aerial ISAC platforms in 6G present two fundamental research challenges. First, unlike terrestrial systems, UAV-aided ISAC is constrained by both limited radio resources and restricted on-board energy supply, due to the size, weight, and power limitations of UAVs [5]. Second, the performance of practical ISAC systems is often impaired by undesired clutter scatters, such as trees, buildings, and vehicles, whose reflected echoes are difficult to distinguish from those of the intended sensing targets. The clutter can severely degrade the reliability of target detection and the accuracy of estimation tasks, as the clutter’s reflected signal power is comparable to or even dominates the received echoes, presenting a significant challenge for ISAC [1], [6]. Developing resource- and energy-efficient UAV-aided ISAC solutions in cluttered environments remains a critical research challenge.

To address this challenge, joint beamforming optimization and trajectory design for UAV-aided ISAC has been explored

in the literature to optimize communication throughput [7], [8], sensing beamforming gain [3], [9], or energy consumption [10]. For instance, in [7], the authors optimized the UAV’s flight trajectory and transmit beamforming to maximize the achievable communication rate while maintaining sufficient beam pattern gain on sensing targets. In [10], the focus was on optimizing transmit beamforming, UAV trajectory planning, and sensing scheduling to minimize the UAV’s total energy consumption over a given duration, while requiring sensing to be conducted exclusively at fixed locations. However, these studies [3], [7]–[10] typically assume ideal radar sensing environments without considering clutter. Given that clutter is influenced by the transmit signal, transmit beamforming techniques, both without and with the aid of intelligent reflecting surfaces (IRSs), have been proposed in [6] to mitigate clutter effects, assuming prior knowledge of the clutter covariance matrix. But this study focused on terrestrial ISAC scenarios, and to the best of our knowledge, the impact of clutter on UAV-aided ISAC has not yet been investigated in the literature.

This paper fills in the research gap by investigating UAV-aided ISAC in a cluttered environment. Unlike previous studies [6], our approach not only integrates transmit beamforming with sensing scheduling, but also exploits the UAV’s mobility to jointly mitigate the impact of clutter during ISAC. Considering the UAV’s flight energy consumption, we further optimize the UAV’s trajectory, transmit beamforming, and sensing scheduling to minimize the UAV’s total energy consumption while guaranteeing quality-of-service (QoS) requirements for both communication and sensing, specifically in terms of achievable data rates and signal-to-clutter-plus-noise ratio (SCNR). Our contributions are

- We investigate the joint optimization of trajectory design, transmit beamforming, and sensing scheduling for performing UAV-enabled ISAC mission in a cluttered environment. The aim is to minimize the UAV’s overall energy consumption during the mission while satisfying communication, sensing and flight requirements.
- The formulated problem is a nonconvex mixed-integer nonlinear program (MINLP). By reformulating it as a multi-stage dynamic program (DP), we propose a novel efficient solution based on the one-step lookahead rollout (OSLR) technique from approximate DP and semidefinite programming (SDP) from convex optimization.
- Simulation results show that the proposed OSLR algorithm can effectively exploit the UAV mobility and multi-antenna beamforming to mitigate the impact of the clutter interference and ensure the sensing and communication QoS requirements at a low energy consumption.

Notations: Throughout this paper, matrices and vectors are denoted by boldface capital and lower-case letters, respectively. \mathbf{A}^T , \mathbf{A}^H , $\text{Rank}(\mathbf{A})$, and $\text{Tr}(\mathbf{A})$ denote the transpose, Hermitian (or conjugate transpose), rank, and trace of matrix \mathbf{A} , respectively. Finally, $|\cdot|$ and $\|\cdot\|$ denote the absolute value of a complex scalar and the Euclidean norm of a complex vector, respectively.

II. SYSTEM MODEL

In this section, we present the channel and signal models for UAV-aided ISAC in a cluttered environment. We also introduce

This work has been funded by the LOEWE initiative (Hesse, Germany) within the emergenCITY center under grant LOEWE/1/12/519/03/05.001(0016)/72 and has been supported by the BMBF project Open6GHub under grant 16KISKO14 and by DAAD with funds from the German Federal Ministry of Education and Research (BMBF).

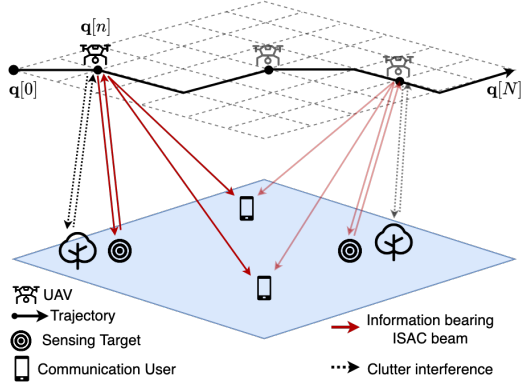


Fig. 1. Illustration of UAV-enabled ISAC to simultaneously detect targets and communicates to multiple users on its trajectory, in presence of undesired clutter scatters.

the performance metrics for sensing and communication and assess the UAV's energy consumption.

A. UAV-aided ISAC in Cluttered Environment

We consider an ISAC system enabled by a rotary-wing UAV. As illustrated in Fig. 1, the UAV is tasked with serving K downlink communication users (CU) and sensing M potential targets (ST) within a cluttered environment containing L unwanted scatters. The UAV is equipped with a full-duplex ISAC transceiver containing S transmit antennas and S receive antennas, both arranged in ULAs. Sensing and communication signals are sent using the same transmit ULA and time-frequency resources, while the receive ULA is used to collect echo signals backscattered to the UAV. Following [11], [12], we assume sufficient separation between the transmit and receive ULAs (or with the aid of additional advanced interference cancellation solutions) to effectively suppress self-interference. The locations of the CUs, STs and the clutter objects, denoted by $\mathbf{u}_k^c \in \mathbb{R}^{2 \times 1}$, $k = 1, \dots, K$, $\mathbf{u}_m^s \in \mathbb{R}^{2 \times 1}$, $m = 1, \dots, M$, and $\mathbf{u}_l^o \in \mathbb{R}^{2 \times 1}$, $l = 1, \dots, L$, respectively, are assumed to be fixed and known to the UAV.

To facilitate trajectory planning, we assume that the UAV flies at a fixed altitude H . Moreover, the flight area is discretized into a uniform grid with G grid vertices indexed by the set $\mathcal{V} \triangleq \{\mathbf{v}_1, \dots, \mathbf{v}_G\} \in \mathbb{R}^{2 \times 1}$. The UAV's flight path consists of $N+1$ waypoints $\mathbf{q}[n] \in \mathcal{V}$, $n = 0, \dots, N$, selected from \mathcal{V} . We assume that the UAV flies at a constant speed for a duration of $\tau[n] > 0$ on the line-segment connecting waypoints $\mathbf{q}[n-1]$ and $\mathbf{q}[n]$. In this paper, the parameters G and N are predetermined, while $\tau[n]$ is a variable to be optimized. The length of line-segment n , given as $\delta[n] = \|\mathbf{q}[n] - \mathbf{q}[n-1]\|$, does not exceed Δ_{\max} . We assume $\Delta_{\max} \ll H$ such that the distances between the UAV and targets remain approximately constant while the UAV flies on each line-segment.

B. 3D Channel and Signal Models for UAV-aided ISAC

The clutter scatters induce multipath propagation for the communication signals. However, as the line-of-sight (LoS) path remains dominant for the elevated UAV, the multipath components are negligible. Consequently, we model the channel vector $\mathbf{h}_k^{\text{tx}}[n]$ from the UAV on line-segment n to CU k as

$$\mathbf{h}_k^{\text{tx}}[n] = \frac{\sqrt{\beta}}{\sqrt{\|\mathbf{u}_k^c - \mathbf{q}[n]\|^2 + H^2}} \cdot \mathbf{a}_k^{\text{tx}}[n], \quad (1)$$

where β denotes the channel power gain at a unit distance. The channel vectors $\mathbf{h}_m^{\text{tx}}[n]$ and $\mathbf{h}_l^{\text{tx}}[n]$ from the UAV to ST m and clutter l are defined in the same manner as $\mathbf{h}_k^{\text{tx}}[n]$ in (1).

Moreover, $\mathbf{a}_k^{\text{tx}}[n]$ is the steering vector of the transmit ULA on line-segment n toward CU k , defined as

$$\mathbf{a}_k^{\text{tx}}[n] \triangleq [1, e^{j\frac{2\pi d}{\lambda} \cos(\theta_k^{\text{tx}}[n])}, \dots, e^{j\frac{2\pi(S-1)d}{\lambda} \cos(\theta_k^{\text{tx}}[n])}]^T. \quad (2)$$

Assume that the axes of the UAV's ULAs are vertically deployed [3], [9]. Then the angle of departures (AoDs) of the CUs, STs, and clutter scatters coincide with their elevation angles from the UAV. Hence, in (2), the AoD for CU k is given as $\theta_k^{\text{tx}}[n] = \arctan(\|\mathbf{u}_k^c - \mathbf{q}[n]\|/H)$. Note that, as $\Delta_{\max} \ll H$, the steering vectors and the channels between the UAV and each CU/ST also remain unchanged when the UAV flies on each line-segment.

Let $s_i \in \mathbb{C}$ be the information bearing symbol intended for CU i . We assume that s_i is a zero-mean complex Gaussian random variable with unit variance. Moreover, let $\mathbf{w}_i \in \mathbb{C}^{S \times 1}$ be the UAV's beamforming vector used for sending s_i . To fully exploit the spatial degrees of freedom (DoFs) provided by the transmit ULA, a dedicated sensing signal $\mathbf{s}_0[n]$ is superimposed with the communication symbols. The resulting ISAC signal transmitted by the UAV on line-segment n is given as $\mathbf{x}[n] = \sum_{i=1}^K \mathbf{w}_i[n] s_i[n] + \mathbf{s}_0[n]$, where $\mathbf{s}_0[n]$ is a zero-mean random vector with covariance matrix $\mathbf{R}_s[n] = \mathbb{E}\{\mathbf{s}_0[n] \mathbf{s}_0^H[n]\}$. The sensing signal $\mathbf{s}_0[n]$ is generated independent of the communication symbols, ensuring that the sensing and communication symbols are mutually uncorrelated. The covariance matrix $\mathbf{R}_x[n]$ of the transmit signal $\mathbf{x}[n]$ is then

$$\mathbf{R}_x[n] = \mathbb{E}\{\mathbf{x}[n] \mathbf{x}^H[n]\} = \sum_{k=1}^K \mathbf{w}_k[n] \mathbf{w}_k^H[n] + \mathbf{R}_s[n]. \quad (3)$$

The received signal at CU k on line-segment n is given as

$$y_k[n] = \sum_{i=1}^K (\mathbf{h}_k^{\text{tx}}[n])^H \mathbf{w}_i[n] s_i[n] + (\mathbf{h}_k^{\text{tx}}[n])^H \mathbf{s}_0[n] + z_k[n], \quad (4)$$

where $z_k[n]$ is the additive white Gaussian noise (AWGN) at CU k and is modeled as a zero-mean Gaussian random variable with variance σ_k^2 . Based on (4), the signal-to-interference-plus-noise ratio (SINR) $\gamma_k[n]$ of CU k is given as

$$\gamma_k[n] = \frac{|\mathbf{h}_k^{\text{tx}}[n])^H \mathbf{w}_k[n]|^2}{\sum_{i=1, i \neq k}^K |(\mathbf{h}_k^{\text{tx}}[n])^H \mathbf{w}_i[n]|^2 + (\mathbf{h}_k^{\text{tx}}[n])^H \mathbf{R}_s[n] \mathbf{h}_k^{\text{tx}}[n] + \sigma_k^2}. \quad (5)$$

Meanwhile, the UAV utilizes the transmit signal $\mathbf{x}[n]$ as a probing signal for radar sensing. The sensing of the multiple targets is scheduled onto different line-segments. Particularly, we define a binary variable $\alpha_m[n] \in \{0, 1\}$ as the indicator for sensing ST m when the UAV flies on line-segment n . The UAV collects echoes of the probing signal that are backscattered by the scheduled ST for tasks such as activity detection and area monitoring based on parameters like AoAs and round-trip times of the echoes [1].

However, the clutter scatters will generate interference for sensing the targets, as their backscattered signals are difficult to distinguish at the ISAC receiver. Note that the clutter scatters do not emit signals of their own. Let $y_m[n]$ and $y_l[n]$ be the signals delivered to ST m and clutter l , respectively, which can be modeled similar to (4). The received signal at the UAV on line-segment n is a collection of echos reflected from the both STs and clutters, i.e.,

$$\mathbf{y}[n] = \sum_{m=1}^M \epsilon_m \mathbf{h}_m^{\text{rx}}[n] y_m[n] + \sum_{l=1}^L \epsilon_l \mathbf{h}_l^{\text{rx}}[n] y_l[n] + \mathbf{z}[n], \quad (6)$$

where ϵ_m and ϵ_l are the reflection coefficients. $\mathbf{h}_m^{\text{rx}}[n]$ and $\mathbf{h}_l^{\text{rx}}[n]$ are the backscattering channel vectors from ST m and

clutter l to the UAV, respectively, defined in the same manner as $\mathbf{h}_k^{\text{tx}}[n]$ in (1). $\mathbf{z}[n]$ is the AWGN with variance σ^2/S at the UAV's receive ULA.

Given the influence of clutter on sensing, the SCNR is a key metric for assessing the accuracy of target detection and localization, as it quantifies the radar's capability to distinguish the target from the clutter interference [1]. Let $\mathbf{H}_m[n] \triangleq \mathbf{h}_m^{\text{tx}}[n](\mathbf{h}_m^{\text{rx}}[n])^H$ and $\mathbf{H}_l[n] \triangleq \mathbf{h}_l^{\text{tx}}[n](\mathbf{h}_l^{\text{rx}}[n])^H$ be the round-trip channel matrices of ST m and clutter l on line-segment n , respectively. When $\alpha_m[n] = 1$, the SCNR $\Gamma_m[n]$ of sensing ST m at the UAV on line-segment n is given as [1]

$$\Gamma_m[n] = \frac{\epsilon_m \text{tr}(\mathbf{H}_m^2[n] \mathbf{R}_x[n])}{\sum_{i=1, i \neq m}^M \epsilon_i \text{tr}(\mathbf{H}_i^2[n] \mathbf{R}_x[n]) + \sum_{l=1}^L \epsilon_l \text{tr}(\mathbf{H}_l^2[n] \mathbf{R}_x[n]) + \sigma^2}. \quad (7)$$

The first and the second term in the denominator of (7) capture the interference from echo signals backscattered from other STs and the clutters, respectively.

C. Energy Consumption of the UAV

During the ISAC mission, the UAV consumes energy in both signal transmission and flight propulsion. The UAV's energy consumption for signal transmission on line-segment n , denoted by $E^c[n]$, is given as

$$E^c[n] = (\text{tr}(\mathbf{R}_x[n]) + P_{\text{const}}) \cdot \tau[n], \quad (8)$$

where $\text{tr}(\mathbf{R}_x[n])$ gives the transmit power and P_{const} is the constant power consumed in the circuitry and signal processing. Meanwhile, the UAV's propulsion consumption between waypoints $\mathbf{q}[n-1]$ and $\mathbf{q}[n]$ is a function of line-segment length $\delta[n]$ and flight duration $\tau[n]$ given as $E^f[n] = E_1^f[n] + E_2^f[n]$ [5], where

$$\begin{aligned} E_1^f[n] &= P_0 \left(1 + \frac{3\delta^2[n]}{U_{\text{tip}}^2 \tau[n]} \right) + \frac{1}{2} d_0 \rho s A \frac{\delta^3[n]}{\tau^2[n]}, \\ E_2^f[n] &= P_i \left(\sqrt{\tau^4[n] + \frac{\delta^4[n]}{4V_0^4}} - \frac{\delta^2[n]}{2V_0^2} \right)^{1/2}. \end{aligned} \quad (9)$$

In (9), the parameters are defined as follows: rotor disc area A , tip speed of the rotor blade U_{tip} , rotor solidity s , air density ρ , fuselage drag ratio d_0 , mean rotor velocity induced in forward flight V_0 , blade profile power during hovering P_0 , and induced power during hovering P_i , cf. [5].

Note that the second term in (9) is a nonconvex function of $\tau[n]$, rendering its optimization difficult. To overcome this challenge, we employ the first-order Taylor approximation $\sqrt{1+x} \approx 1 + \frac{1}{2}x$ for $|x| \ll 1$ and approximate $E_2^f[n]$ as

$$E_2^f[n] \approx \frac{P_i V_0 \tau^2[n]}{\delta[n]}. \quad (10)$$

In (10), $E^f[n]$ is a jointly convex function of $\tau[n]$ and $\delta[n]$, but not jointly convex with respect to $\tau[n]$ and $\mathbf{q}[n]$.

III. PROBLEM FORMULATION

To efficiently utilize the UAV's mobility and available radio resources for performing ISAC in the clutter environment, in this section, we jointly optimize the transmit beamforming vectors $\{\mathbf{w}_k[n]\}$, sensing covariance matrices $\{\mathbf{R}_s[n]\}$, sensing schedule $\{\alpha_m[n]\}$, and the UAV's flight trajectory $\{\mathbf{q}[n], \tau[n]\}$ for minimizing the UAV's energy consumption,

while satisfying the QoS requirements for both communication and sensing. The optimization problem is formulated as

$$\begin{aligned} \text{P1: } & \min_{\substack{\mathbf{q}[n], \mathbf{w}_k[n], \mathbf{R}_s[n], \\ \alpha_m[n], \tau[n]}} \sum_{n=1}^N (E^c[n] + E^f[n]) \quad (11) \\ \text{s.t. C1: } & \Gamma_m[n] \geq \alpha_m[n] \Gamma_{\min}, \quad \forall m, \forall n \\ \text{C2: } & \sum_{n=1}^N \alpha_m[n] \tau[n] \geq \alpha_{\min}, \quad \forall m \\ \text{C3: } & \alpha_m[n] \in \{0, 1\}, \quad \forall m, \forall n \\ \text{C4: } & \gamma_k[n] \geq \gamma_{\min, k}, \quad \forall k, \forall n \\ \text{C5: } & \sum_{k=1}^K \mathbf{w}_k^H[n] \mathbf{w}_k[n] + \text{tr}(\mathbf{R}_s[n]) \leq P_{\max}, \quad \forall n \\ \text{C6: } & \|\mathbf{q}[n] - \mathbf{q}[n-1]\| / \tau[n] \leq V_{\max}, \quad \tau[n] \geq 0, \quad \forall n \\ \text{C7: } & \mathbf{q}[0] = \mathbf{q}_I, \quad \mathbf{q}[N] = \mathbf{q}_F, \quad \mathbf{q}[n] \in \mathcal{V}, \quad \forall n \\ \text{C8: } & \|\mathbf{q}[n] - \mathbf{q}[n-1]\| \leq \Delta_{\max}, \quad \forall n. \end{aligned}$$

In problem P1, constraint C1 ensures that the echoes backscattered from the STs meets a minimum SCNR requirement, even in the presence of clutter. C2 guarantees that each ST is allocated at least α_{\min} amount of sensing time in total, in order to collect a sufficient number of samples for the sensing task. C3 is the binary constraint on sensing scheduling. C4 ensures that the instantaneous SINR of the CUs remains above the threshold $\gamma_{\min, k}$, thereby achieving a minimum data rate of $\log_2(1 + \gamma_{\min, k})$ in bps/Hz during communication. C5 limits the maximum transmit power of the transmit ULA to P_{\max} . C6 limits the UAV's flight velocity. Finally, C7 and C8 specify the UAV's initial, final, and other waypoints on its flight trajectory, subject to a maximal length of line-segments.

Problem P1 is a nonconvex MINLP due to the discrete variables $\mathbf{q}[n]$ and $\alpha_m[n]$, cf. constraints C7 and C3, the nonconvex objective function, and the nonconvex constraints C1, C2, and C4. Moreover, the UAV's trajectory $\mathbf{q}[n]$ is tightly coupled with the transmit beamforming vector $\mathbf{w}_k[n]$ and the sensing covariance matrix $\mathbf{R}_s[n]$, cf. (5) and (7). Similar tight couplings also exist between flight duration $\tau[n]$ and other optimization variables, cf. (8)–(9) and C2. These obstacles render problem P1 generally intractable. To overcome these challenges, in Sec. IV we reformulate P1 as a multi-stage DP, whose optimal solution is given by the Bellman optimality equation. However, solving this equation exactly using standard DP algorithms requires prohibitive computational complexity. Inspired by the success of approximate DP and reinforcement learning, we propose a low-complexity, high-quality suboptimal algorithm based on the rollout method [13] to obtain an approximate solution to the Bellman equation.

IV. PROPOSED SOLUTION

A. Optimization of Transmit Beamforming, Sensing Covariance Matrix, and Flight Duration

We start with optimizing the continuous-valued beamforming vectors \mathbf{w}_k , sensing covariance matrices \mathbf{R}_s , and flight duration $\tau[n]$, while assuming that the discrete-valued waypoints $\mathbf{q}[n]$ and sensing schedule $\alpha_m[n]$ are given. The optimization problem is given as,

$$\begin{aligned} \text{P2: } & \min_{\substack{\mathbf{w}_k[n], \mathbf{R}_s[n], \tau[n]}} \sum_{n=1}^N (E^c[n] + E^f[n]) \quad (12) \\ \text{s.t. } & \text{C1, C2, C4, C5, C6, C8.} \end{aligned}$$

Problem P2 is nonconvex due to its nonconvex objective function and nonconvex constraints C1, C2, and C4. However, using appropriate transformation techniques, we uncover an

underlying convexity within P2. Consequently, the globally optimal solution of P2 can be obtained within polynomial-time computational complexity. This property further enables us to tackle the remaining optimization of discrete variables using DP-based approaches in Secs. IV-B and IV-C.

1) *Problem Transformation*: Let us define new variables $\mathbf{W}_k[n] \triangleq \tau[n]\mathbf{w}_k[n]\mathbf{w}_k^H[n]$ and $\bar{\mathbf{R}}_s[n] \triangleq \mathbf{R}_s[n]\tau[n]$, where $\mathbf{W}_k[n] \succeq 0$ and $\text{Rank}(\mathbf{W}_k[n]) \leq 1$. Using $\mathbf{W}_k[n]$ and $\bar{\mathbf{R}}_s$ to eliminate \mathbf{w}_k and \mathbf{R}_s , we can rewrite C4 as

$$\frac{|(\mathbf{h}_k^{\text{tx}}[n])^H \mathbf{w}_k[n]|^2}{\sum_{i \neq k} |(\mathbf{h}_i^{\text{tx}}[n])^H \mathbf{w}_i[n]|^2 + (\mathbf{h}_k^{\text{tx}}[n])^H \bar{\mathbf{R}}_s[n] \mathbf{h}_k^{\text{tx}}[n] + \sigma_k^2} \geq \gamma_{\min, k}$$

$$\iff \bar{\text{C4}}: (1 + \gamma_{\min, k}^{-1}) \text{tr}(\mathbf{W}_k[n] \mathbf{H}_k[n]) - \text{tr}(\bar{\mathbf{R}}_x[n] \mathbf{H}_k[n]) \geq \sigma_k^2 \tau[n], \quad (13)$$

where $\bar{\mathbf{R}}_x[n] \triangleq \mathbf{R}_x[n]\tau[n] = \sum_{k=1}^K \mathbf{W}_k[n] + \bar{\mathbf{R}}_s[n]$, and $\mathbf{H}_k[n] \triangleq \mathbf{h}_k^{\text{tx}}[n](\mathbf{h}_k^{\text{tx}}[n])^H$. Similarly, we reformulate C1 as

$$\text{C1} \iff \bar{\text{C1}}: \bar{\Gamma}_m[n] \geq \tau[n] \alpha_m[n] \Gamma_{\min}, \quad \text{with}$$

$$\bar{\Gamma}_m[n] = \frac{\epsilon_m \text{tr}(\mathbf{H}_m^2[n] \bar{\mathbf{R}}_x[n])}{\sum_{i \neq m} \epsilon_i \text{tr}(\mathbf{H}_i^2[n] \bar{\mathbf{R}}_x[n]) + \sum_{l=1}^L \epsilon_l \text{tr}(\mathbf{H}_l^2[n] \bar{\mathbf{R}}_x[n]) + \sigma^2}.$$

Therefore, given the waypoints $\mathbf{q}[n]$ and sensing schedule $\alpha_m[n]$, problem P2 can be equivalently reformulated as:

$$\text{P3:} \quad \min_{\mathbf{W}_k[n], \bar{\mathbf{R}}_x[n], \tau[n]} \sum_{n=1}^N (E^c(\bar{\mathbf{R}}_x[n]) + E^f(\tau[n])) \quad (14)$$

s.t. $\bar{\text{C1}}, \bar{\text{C2}}, \bar{\text{C4}}, \bar{\text{C5}}, \bar{\text{C6}}, \bar{\text{C8}}$

$$\text{C9: } \mathbf{W}_k[n] \succeq 0, \forall n, \forall k$$

$$\text{C10: } \text{Rank}(\mathbf{W}_k[n]) \leq 1, \forall n, \forall k.$$

2) *Hidden Convexity and Optimal Solution*: If constraint C10 is eliminated from P3, it results in a relaxed problem that is a convex SDP and can be optimally solved using off-the-shelf solvers such as CVX [14]. In general, this relaxation provides a lower bound for the optimal objective value of problem P3, as the relaxed solution may not satisfy constraint C10. However, for problem P3 at hand, we can show that the relaxed solution of \mathbf{W}_k always has rank one, that is, the relaxed objective value is as *tight* as the optimal value. This finding has also been validated offline by simulations.

Lemma 1: Assume that problem P3 is *strictly* feasible, i.e., it has at least a feasible solution satisfying one of its constraints with strict inequality. Then, the optimal solution of $\mathbf{W}_k[n]$ obtained by SDP relaxation always has rank one. Moreover, the optimal beamforming solution of problem P3 is given by the principal eigenvector of $\mathbf{W}_k[n]/\tau[n]$.

Proof: Due to the limited page space, we only provide a sketch of the proof. When problem P3 is strictly feasible, the convex SDP obtained by relaxing constraint C10 fulfills the Slater's condition and thus has strong duality. As a result, the Karush–Kuhn–Tucker (KKT) conditions are both sufficient and necessary for the optimal relaxed solutions. Following similar arguments in [15, Theorem 2], we can show that the optimal solution of $\mathbf{W}_k[n]$ derived from the KKT conditions always has rank one. Thus, the optimal transmit covariance matrix of problem P3 is given by $\mathbf{W}_k[n]/\tau[n]$, which completes the proof. ■

B. DP based Optimal Solution of Problem P1

We further show below that problem P1 can be reformulated as an equivalent N -stage DP problem and thereby optimally solved via DP algorithms.

1) *DP Reformulation*: With a slight abuse of notation, let n also be the index of stages. Let $\alpha_{\mathcal{M}}[n]$ be the sensing schedule for all STs, indexed by set $\mathcal{M} \triangleq \{1, \dots, M\}$, at stage n . The system state $\mathbf{o}_n \triangleq [Q_n, A_n]$ consists of the sequence of waypoints $Q_n \triangleq \{\mathbf{q}[0], \dots, \mathbf{q}[n]\}$ visited by the UAV and the sensing schedules $A_n = \{\alpha_{\mathcal{M}}[1], \dots, \alpha_{\mathcal{M}}[n]\}$ up to stage n . The action $\mathbf{z}_n = (\mathbf{q}[n+1], \alpha_{\mathcal{M}}[n+1])$ includes the next waypoint $\mathbf{q}[n+1]$ and sensing schedule $\alpha_{\mathcal{M}}[n+1]$ for the next waypoint. The action \mathbf{z}_n must lie in a subset $\mathcal{Z}(\mathbf{o}_n)$ determined by the current state \mathbf{o}_n and the constraints specified in P1.

By applying action \mathbf{z}_n at stage n , the system state evolves to the next state \mathbf{o}_{n+1} according to $\mathbf{o}_{n+1} = f_n(\mathbf{o}_n, \mathbf{z}_n)$, where $f_n(\cdot)$ is essentially the union operator. A cost $g_n(\mathbf{o}_n, \mathbf{z}_n)$ is generated for the transition from \mathbf{o}_n to \mathbf{o}_{n+1} under action \mathbf{z}_n . The cost $g_n(\mathbf{o}_n, \mathbf{z}_n) \triangleq E_{n+1} - E_n$ represents the increase in the UAV's energy consumption, where E_n denotes the total energy consumed up to stage n . To compute E_n , we solve the convex decoupled problem P3 with \mathbf{o}_n as the fixed discrete variables, as described in IV-A.

For the entire ISAC mission, the actions $\mathbf{z}_n, n=0, \dots, N-1$, are determined by a policy $\pi = \{\mu_0, \dots, \mu_{N-1}\}$, where μ_n maps states \mathbf{o}_n into actions $\mathbf{z}_n = \mu_n(\mathbf{o}_n)$. Given an initial state $\mathbf{o}_0 = [Q_0 = \{\mathbf{q}_I\}, A_n = \emptyset]$ and policy π , the total cost of the ISAC mission is $J_\pi(\mathbf{o}_0) = g_N(\mathbf{o}_N) + \sum_{n=0}^{N-1} g_n(\mathbf{o}_n, \mathbf{z}_n)$, which corresponds to energy consumed by the UAV for flight and ISAC. Thus, problem P1 is equivalent to finding the optimal policy denoted by π^* , that minimizes $J_\pi(\mathbf{o}_0)$ [16].

2) *Bellman Optimality Equation*: Let $J_{n, \pi^*}^*(\mathbf{o}_n)$ be the optimal value function of state \mathbf{o}_n , which evaluates the optimal cost to reach state \mathbf{o}_N from state \mathbf{o}_n . Then, the optimal policy π^* is given by the solution of the Bellman optimality equation at each stage $n=0, \dots, N-1$ [16]:

$$J_{n, \pi^*}^*(\mathbf{o}_n) = \min_{\mathbf{z}_n \in \mathcal{Z}_n(\mathbf{o}_n)} [g_n(\mathbf{o}_n, \mathbf{z}_n) + J_{n+1, \pi^*}^*(f(\mathbf{o}_n, \mathbf{z}_n))]. \quad (15)$$

The exact solution to (15) can be obtained using the DP algorithm. It starts with solving problem $J_{N, \pi^*}^*(\mathbf{o}_N)$ at the terminal stage and then moves backwards to solve $J_{N-1, \pi^*}^*(\mathbf{o}_{N-1}), \dots, J_0^*(\mathbf{o}_0)$ stage-wise. The optimal policy is then reconstructed based on the optimal value functions.

However, the DP algorithm is prohibitively time-consuming, due to the exponential growth in state-space with the number of stages, N [16]. This motivates the use of low-complexity approximation methods, such as the rollout algorithm [13], to address (15).

C. Proposed One-Step Lookahead Rollout (OSLR) Algorithm

In the DP algorithm, calculating the optimal value function J_{n+1, π^*}^* is computationally intensive. To lower the computational complexity, the OSLR algorithm approximates J_{n+1, π^*}^* with the value function $\tilde{J}_{n+1, \tilde{\pi}}$ of a *base policy* $\tilde{\pi} = \{\tilde{\mu}_0, \dots, \tilde{\mu}_{N-1}\}$. The base policy $\tilde{\pi}$ can be any heuristic algorithm with an easy-to-compute cost function \tilde{g}_n such that

$$\tilde{J}_{n+1, \tilde{\pi}}(\mathbf{o}_{n+1}) \triangleq \tilde{g}_N(\mathbf{o}_N) + \sum_{i=n+1}^{N-1} \tilde{g}_i(\mathbf{o}_i, \tilde{\mathbf{z}}_i) \quad (16)$$

for $\tilde{\mathbf{z}}_i = \tilde{\mu}_i(\mathbf{o}_i), i = n+1, \dots, N-1$. Substituting J_{n+1, π^*}^* in (15) by $\tilde{J}_{n+1, \tilde{\pi}}$, the action \mathbf{z}_n^+ is selected using OSLR as

$$\mathbf{z}_n^+ \in \underset{\mathbf{z}_n \in \mathcal{Z}(\mathbf{o}_n)}{\text{argmin}} \left[g_n(\mathbf{o}_n, \mathbf{z}_n) + \tilde{J}_{n+1, \tilde{\pi}}(f(\mathbf{o}_n, \mathbf{z}_n)) \right]. \quad (17)$$

TABLE I
PARAMETER SETTINGS FOR SIMULATION

Parameter	Notation/Value
UAV path discretization	$N = 50, \Delta_{\max} = 17$ m
UAV's flight altitude	$H = 100$ m
UAV's max flight speed	$V_{\max} = 20$ m/s
Number of ULA elements	$S = 8$
Reference channel gain	$\beta = -30$ dB
Noise power	$\sigma_k^2 = -110$ dBm
Maximum transmit power	$P_{\max} = 30$ dBm
Circuitry power consumption	$P_{\text{const}} = 5$ W
Flight power parameters [5]	$A = 0.503$ m ² , $P_0 = 80$ W, $P_i = 88.6$ W, $U_{\text{tip}} = 120$ m/s, $\rho = 1.225$ kg/m, $s = 0.05$ m ³ , $d_0 = 0.6$, $V_0 = 4.03$
Communication SINR	$\gamma_{\min,k} = 16$ dB
Sensing SCNR	$\Gamma_{\min,m} = -4$ dB
Sensing duration	$\alpha_{\min} = 3$ s

That is, instead of directly taking actions specified by base policy $\tilde{\pi}$, the OSLR approach optimizes the action by considering both the immediate cost $g_n(\mathbf{o}_n, \mathbf{z}_n)$ and an approximate long-term cost \tilde{J}_{n+1} in each iteration. The solution obtained by (17) is guaranteed with an improved performance over the original base policy while keeping computational costs low [13].

Algorithm 1 presents the proposed OSLR algorithm. At each stage n , the action subset $\mathcal{Z}(\mathbf{o}_n)$ is first determined based on the current state \mathbf{o}_n and the constraints specified in P1. Next, $\tilde{J}_{n+1, \tilde{\pi}}(\mathbf{o}_n, \mathbf{z}_n)$ is computed using the base policy $\tilde{\pi}$ for all $\mathbf{z}_n \in \mathcal{Z}(\mathbf{o}_n)$. Then, the improved action \mathbf{z}_n^+ is determined by solving the convex problem P3 and comparing the resulting energy costs of actions. Finally, the state is updated with the action \mathbf{z}_n^+ that minimizes the energy cost. This process iterates through N stages, yielding a sequence of trajectory waypoints and sensing schedules to minimize the UAV's energy cost for the ISAC mission.

Algorithm 1 Joint Trajectory, Beamforming, and Scheduling Optimization with OSLR

- 1: **Input:** $N, \tilde{\pi}, V_{\max}, P_{\max}, \mathbf{q}_I, \mathbf{q}_F, \{\mathbf{u}_k^c, \gamma_{\min,k}\}_{k=1}^K, \{\mathbf{u}_m^s, \Gamma_{\min,k}, \alpha_{\min}\}_{m=1}^M$
- 2: **for** $n = 0 : N - 1$ **do** ▷ For each stage n
- 3: Initialize $\mathcal{Z}(\mathbf{o}_n)$ ▷ Constraints P1
- 4: Calculate $\tilde{J}_{n+1, \tilde{\pi}}(f(\mathbf{o}_n, \mathbf{z}_n)), \forall \mathbf{z}_n \in \mathcal{Z}(\mathbf{o}_n)$
- 5: $\mathbf{z}_n^+ = \underset{\mathbf{z}_n \in \mathcal{Z}(\mathbf{o}_n)}{\text{argmin}} [g_n(\mathbf{o}_n, \mathbf{z}_n) + \tilde{J}_{n+1, \tilde{\pi}}(\mathbf{o}_n, \mathbf{z}_n)]$
- 6: Update system: $\mathbf{o}_{n+1} = f_n(\mathbf{o}_n, \mathbf{z}_n^+)$ ▷ Solve P3
- 7: **end for**
- 8: **Output:** $[\mathbf{z}_0^+, \dots, \mathbf{z}_{N-1}^+, J_0^+(\mathbf{o}_0)]$.

V. SIMULATION RESULTS

We evaluate the performance of the proposed algorithm via simulations. The UAV performs ISAC within a cluttered area of $500\text{m} \times 500\text{m}$ in size. The area is divided into a uniform grid with 41×41 nodes. We consider $K=2$ CUs located at $[126\text{m}, 151\text{m}]$ and $[374\text{m}, 376\text{m}]$, and $M=2$ STs located at $[151\text{m}, 374\text{m}]$ and $[401\text{m}, 126\text{m}]$. Additionally, $L=8$ clutter elements are placed around the STs at various distances. The UAV's initial and final waypoints are set as $\mathbf{q}_I=[25\text{m}, 250\text{m}]$ and $\mathbf{q}_F=[500\text{m}, 225\text{m}]$, respectively. Unless otherwise stated, the simulation parameters are set as in Table I.

To validate the effectiveness of Algorithm 1, Fig. 2 illustrates the evolution of the *estimated energy cost*, given by the sum of accumulated and future energy costs $\sum_{i=0}^{n-1} g_i(\mathbf{o}_i, \mathbf{z}_i^+) + \tilde{J}_{n, \tilde{\pi}}(\mathbf{o}_n)$, at each stage $n=1, \dots, N$, where the action \mathbf{z}_i^+ is

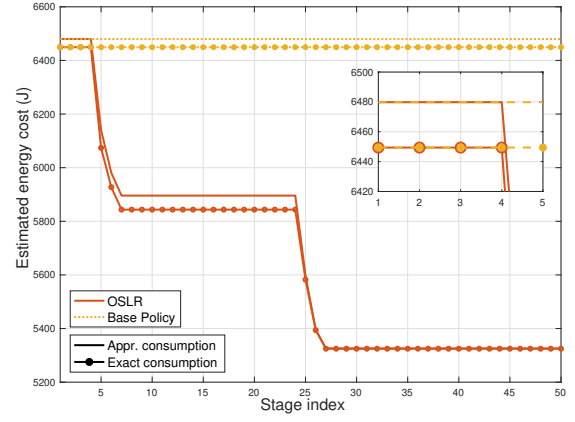


Fig. 2. Iterative performance of proposed OSLR algorithm over N stages.

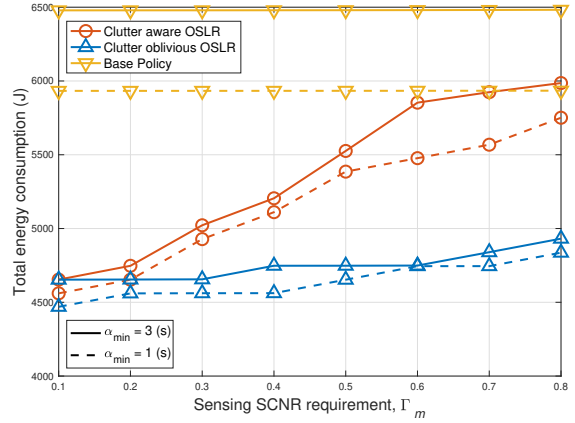


Fig. 3. UAV energy consumption versus the required sensing SCNR per ST defined in (17). The OSLR step in Algorithm 1 employs the fly-hover-and-sense protocol in [10] as *base policy*, where the UAV only performs sensing while hovering above the STs, for minimizing clutter effects and improving sensing quality. For comparison, the estimated energy costs of the base policy, i.e., $\sum_{i=0}^{n-1} g_i(\mathbf{o}_i, \tilde{\mathbf{z}}_i) + \tilde{J}_{n, \tilde{\pi}}(\mathbf{o}_n)$, are also evaluated, where the action $\tilde{\mathbf{z}}_i$ is specified by the *base policy*. As expected, the estimated energy costs of the base policy do not change over stages, since all actions are predetermined. In contrast, by optimizing its actions at each stage based on both the immediate and potential long-term costs in (17), the OSLR method can successively improve the performance over the *base policy*. Additionally, Figure 2 compares the “Approximate” and “Exact” energy consumption curves, calculated using (10) and (9), respectively, for the same solution obtained by Algorithm 1 or its base policy. The close alignment of these two curves validates that the approximation in (10) is practically tight. However, as the actual energy consumption function in (9) is nonconvex, it is difficult to evaluate the loss associated with optimizing the approximate energy consumption model (10) rather than (9).

Fig. 3 depicts the UAV's energy consumption versus the sensing SCNR requirement per ST, $\Gamma_{\min,m}$ for the proposed “Clutter-aware OSLR” scheme, the *base policy* $\tilde{\pi}$, and a “Clutter-oblivious OSLR” scheme, which uses the OSLR algorithm for joint beamforming, sensing scheduling, and trajectory design but ignores the clutter effect in (7). We observe that, unlike the base policy, the energy consumption of both the proposed and “Clutter-oblivious OSLR” schemes increase monotonically with $\Gamma_{\min,m}$. Moreover, the proposed scheme significantly outperforms the base policy, particularly for small $\Gamma_{\min,m}$ s, by sensing farther from STs and shortening

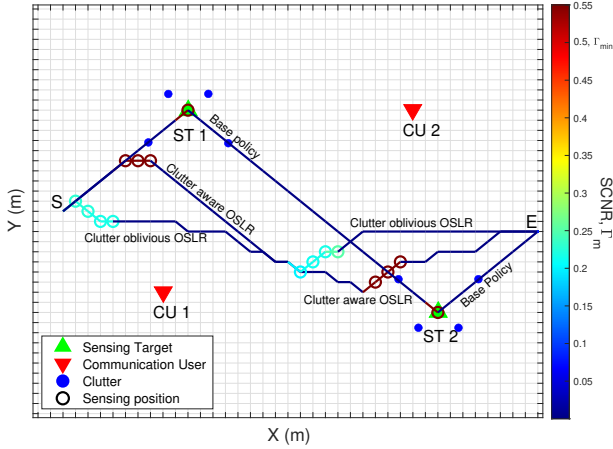


Fig. 4. Optimized flight trajectories of the UAV for the considered schemes, where the SCNRs at different sensing positions are indicated in color according to the color map next to the figure.

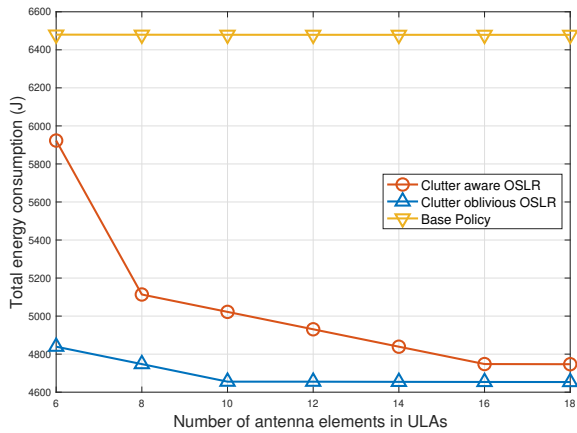


Fig. 5. UAV energy consumption versus the number of transmit antennas.

the flight path according to SCNR requirements. However, as $\Gamma_{\min, m}$ increases, the proposed scheme consumes significantly more energy than the “Clutter-oblivious OSLR” scheme. This is because, with the proposed scheme, the UAV needs to fly closer to the ST locations to mitigate the clutter interference and meet the more stringent requirements on sensing SCNR. However, sensing QoS cannot be ensured with the “Clutter-oblivious OSLR” scheme. Additionally, as the allowed sensing duration α_{\min} increases from 1s to 3s, the UAV can schedule the sensing on multiple waypoints during flight with more flexibility. This translates into only a small increase in energy consumption for the proposed scheme.

For further insights, Fig. 4 shows the optimized UAV trajectories and sensing locations (namely those line-segments where $\alpha_m[n] = 1$), when the required minimum sensing SCNR is $\Gamma_{\min} = 0.5$. As expected, the base policy follows a path from the UAV’s initial to final waypoints via the ST locations. This ensures reliable sensing but increases energy consumption, due to a longer trajectory and extended hovering time. In contrast, the proposed scheme adapts its trajectory, sensing schedule, and beamforming to meet sensing requirements efficiently during flight. The “Clutter-oblivious OSLR” scheme senses from waypoints further away from the ST positions, reducing energy consumption with a shorter flight path. However, Fig. 4 shows that ignoring clutter interference significantly diminishes the achievable SCNR during sensing.

Finally, Fig. 5 evaluates the UAV’s energy consumption versus the number of antennas elements in the UAV’s ULAs. We

observe that increasing the number of antennas enhances the performance of the proposed and “Clutter-oblivious OSLR” schemes. Because, with more antennas, the signal energy can be focused towards the STs and CUs using narrower beams, resulting in reduced clutter interference. The base policy remains constant for different antenna settings because it uses the same trajectory in all simulations. In contrast, our proposed scheme jointly optimizes the trajectory design, sensing scheduling, flight times, and ISAC beamforming, which shortens the flight trajectory and saves energy while still meeting the sensing requirements. Thus, the proposed scheme allows the UAV to better utilize the antenna array to increase sensing power towards the STs while mitigating clutter interference.

VI. CONCLUSION

In this paper, we studied the joint optimization of transmit beamforming, sensing scheduling, and trajectory design for UAV-enabled ISAC in cluttered environments. We formulated a highly nonconvex optimization problem aimed at minimizing the UAV’s energy consumption while meeting the QoS requirements for communication and sensing, as well as adhering to flight constraints. By reformulating the problem as a multi-stage DP, we proposed a computationally efficient OSLR algorithm to obtain a high-quality suboptimal solution. Simulation results demonstrated that the proposed scheme can jointly optimize the UAV trajectory and leverage the spatial DoFs of the transmit ULA to significantly reduce UAV’s energy consumption required for ensuring communication and sensing QoS. Motivated by its high performance and low complexity, future work will explore extending the proposed OSLR algorithm to other base policies and multi-UAV enabled ISAC systems.

REFERENCES

- [1] F. Liu et al., “Integrated sensing and communications: Toward dual-functional wireless networks for 6G and beyond,” *IEEE J. Sel. Areas Commun.*, vol. 40, no. 6, pp. 1728–1767, 2022.
- [2] K. Meng et al., “UAV-enabled integrated sensing and communication: Opportunities and challenges,” *IEEE Wireless Commun.*, vol. 31, no. 2, pp. 97–104, 2024.
- [3] M.B. Yilmaz et al., “Joint beamforming and trajectory optimization for UAV-enabled ISAC under a finite energy budget,” in *IEEE ICC Workshops*, 2024.
- [4] M. B. Yilmaz et al., “UAV-assisted delay-sensitive communications with uncertain user locations: a cost minimization approach,” in *Proc. IEEE PIMRC*, 2022.
- [5] Y. Zeng et al., “Energy minimization for wireless communication With rotary-wing UAV,” *IEEE Trans. Wireless Commun.*, vol. 18, no. 4, pp. 2329–2345, 2019.
- [6] C. Liao et al., “Optimized design for IRS-assisted integrated sensing and communication systems in clutter environments,” *IEEE Trans. Commun.*, vol. 71, no. 8, pp. 4721–4734, 2023.
- [7] Z. Lyu et al., “Joint maneuver and beamforming design for UAV-enabled integrated sensing and communication,” *IEEE Trans. Wireless Commun.*, vol. 22, no. 4, pp. 2424–2440, 2023.
- [8] K. Meng et al., “UAV trajectory and beamforming optimization for integrated periodic sensing and communication,” *IEEE Wireless Communications Letters*, vol. 11, no. 6, pp. 1211–1215, 2022.
- [9] M.B. Yilmaz et al., “Joint beamforming and trajectory optimization for UAV-aided ISAC with dipole antenna array,” in *27th International Workshop on Smart Antennas (WSA)*, 2024.
- [10] A. Khalili et al., “Energy-aware resource allocation and trajectory design for UAV-enabled ISAC,” in *Proc. IEEE Globecom*, 2023.
- [11] M. F. Keskin et al., “Limited feedforward waveform design for OFDM dual-functional radar-communications,” *IEEE Trans. Signal Process.*, vol. 69, pp. 2955–2970, 2021.
- [12] J. Kim et al., “On the learning of digital self-interference cancellation in full-duplex radios,” *IEEE Wireless Commun.*, vol. 31, no. 4, pp. 184–191, 2024.
- [13] D. P. Bertsekas, *Lessons from AlphaZero for optimal, model predictive, and adaptive control*. Athena Scientific, 2022.
- [14] M. Grant and S. Boyd, “CVX: Matlab software for disciplined convex programming, version 2.1,” <http://cvxr.com/cvx>, 2014.
- [15] J. Zhang, Y. Zhang et al., “Robust energy-efficient transmission for wireless-powered D2D communication networks,” *IEEE Trans. Veh. Technol.*, vol. 70, no. 8, pp. 7951–7965, 2021.
- [16] D. Bertsekas, *Dynamic programming and optimal control*, 2nd ed. Athena Scientific, 2001, vol. 1 and 2.